Electronic properties of stage-3 $SbCl_5$-intercalated graphite

G. Wang, H. Zaleski, P. K. Ummat, and W. R. Datars
Department of Physics, McMaster University, Hamilton, Ontario, Canada L8S 4M1
(Received 30 November 1987)

The stage-3 antimony pentachloride–graphite intercalated compound has three groups of de Haas–van Alphen (dHvA) frequencies with the magnetic field parallel to the c axis. The dominant frequency from the first group and the two average frequencies from the second and third groups are identified with the basic graphitic bands. These frequencies are used to determine γ_0, γ_1, and δ in Blinowski's band model and to calculate energy bands. The energy differences between the valence bands at the Fermi level are in agreement with the optical-reflectance experimental results of Hoffman *et al.* The predicted cyclotron masses are within 12% of the measured values. The charge distribution along the k_z direction of the three graphite layers of the stage-3 compound is determined to be between the uniform charge distribution and that of metallic sandwich models. This results from the screening effect of the external graphite layers. The splitting of dHvA frequencies in each group is attributed to undulation of the Fermi surface along the k_z direction and to the presence of intercalant islands.

I. INTRODUCTION

Antimony pentachloride ($SbCl_5$) in graphite is one of the most widely studied acceptor intercalants because it is one of the most stable graphite intercalation compounds (GIC) in air.[1,2] A systematic x-ray study[3] of the graphite-$SbCl_5$ system showed the existence of a series of distinct stoichiometric compositions which were identified with different stages. Stage-1–4 intercalation compounds were obtained and their composition was described by the general formula $C_{12n}SbCl_5$ where n is the stage index. In other work[4] stage-2–5 graphite-$SbCl_5$ were synthesized by a two-zone method and optical-reflectance spectra of the compounds were found to remain unchanged after several months of air exposure.

There have been many in-plane structural studies of $SbCl_5$ GIC's using a variety of techniques. The most commonly seen in-plane crystalline structure is a commensurate lattice which is stable from 230 to 425 K.[5] Associated with this structure is an amorphous phase which coalesces into a weakly incommensurate lattice on cooling the sample below 230 K. Electron[6–8] and x-ray[5] diffraction measurements have also detected the incommensurate structure at ambient temperature coexisting with the commensurate structure. As with the commensurate structure, the incommensurate structure undergoes a transition to a glassy phase around 200 K when exposed to an electron beam.[7]

The optical reflectance of the electronic structure of this acceptor-type GIC has been studied by Hoffman *et al.*[9] They measured the absolute reflectance at near-normal incidence of stage-1–4 $SbCl_5$-graphite intercalation compounds in the photon-energy range 0.08–10 eV and determined a variety of parameters relevant to the charge transfer and electronic band structure of these materials, such as the valence-band energy differences near the Brillouin-zone corner, the position of the Fermi level, and the optical mass.

The first measurements of quantum oscillatory phenomena of the $SbCl_5$ compounds were reported by Batallan *et al.*[10] They investigated stages 2 and 4 and found that the frequencies of the oscillations were independent of stage. Later studies by Takahashi *et al.*[11] for stage-2–4 $SbCl_5$-GIC's showed a stage dependence of the dHvA frequencies, but the number of observed frequencies was larger than that expected from the band models of Blinowski *et al.*[12,13] More recently, the measurements of the de Haas–van Alphen (dHvA) effect in the lowest stages of antimony pentachloride–graphite compounds by Zaleski *et al.*[14,15] observed a single dHvA oscillation in the stage-1 compound and two dHvA oscillations in the stage-2 compound. They compared the values of the frequencies and corresponding carrier cyclotron masses with the predictions of rigid-band models. Very good agreement was found with the model of Holzwarth[16] and the simpler model of Blinowski *et al.*[13] was found to be reasonable but less accurate than the Holzwarth model. Its predictions were about 10% different from the measured values. It has also been found that the low-temperature structures of these GIC's are strongly dependent on the rate of cooling.[8,14,15,17] For cooling from room temperature to about 200 K in less than 24 h a very complicated dHvA spectra was obtained for different stages. A slower cooling rate produced very simple dHvA spectra in stage 1 and stage 2.

This work presents the results of the investigations of the electronic bands and charge distribution of the stage-3 acceptor $SbCl_5$-graphite compound by the dHvA effect. The details of sample preparation, x-ray characterization, and the dHvA method are given in Sec. II. In Sec. III, experimental results are presented and some particular phenomena are analyzed. In Sec. IV, experimental data relating to the band structure are compared to the predications of Blinowski's band model[12] and the charge distribution along the c axis is derived. Finally, in Sec. V the results are summarized and the conclusions are presented.

II. EXPERIMENT

For the sample preparation most of the handling was done in a glove box filled with dry nitrogen. The content of the water vapor inside the dry box was less than 1 ppm. The starting material was highly oriented pyrolitic graphite (HOPG). Cylinders of diameter 3 mm were cut from HOPG and cleaved to about 0.5 mm thickness. The outer layers were removed by peeling. The pieces were then washed in acetone in an ultrasonic cleaner. Cleaned HOPG pieces were put into a glass container and dried under vacuum at an elevated temperature.

Antimony pentachloride was purified by three successive trap-to-trap vacuum distillations. Pure $SbCl_5$ was pale yellow in color and was stored in a Pyrex tube that was kept in a dry box.

The samples were prepared by using a two-zone furnace. First, a piece of graphite was put into a Pyrex glass tube which had a constriction in the middle of it. The constriction prevented the sample from dropping down to the bottom. Then the tube was connected to a vacuum line and evacuated for a few hours at an elevated temperature. After that, it was transferred into the dry box where $SbCl_5$ was added to the bottom of the tube. Nitrogen dissolved in antimony pentachloride was removed after taking it out of the dry box by pumping and periodically freezing $SbCl_5$ in the tube with liquid nitrogen. Then, the tube was sealed and put into a two-zone furnace. The temperatures of the graphite and intercalant, T_g and T_i, were 175 and 90 °C, respectively. After 69 h, the reaction was completed, the tube was taken out of the furnace and the bottom of the tube was put into liquid nitrogen. The sample was sealed off after all unreacted $SbCl_5$ condensed in the lower end.

The stage of each sample was determined by x-ray diffraction measurement using a powder diffractometer and Cu $K\alpha$ radiation. A straight line was fit to the reflection order l versus $1/d_l$ determined from the Bragg formula and the value of I_c was calculated from the slope of the line. The c axis repeat distance I_c of the stage-3 compounds was measured to be $I_c = 16.02$ and 16.10 Å for the first and second samples, respectively. They are very close to 16.06 Å, which is expected for this stage.

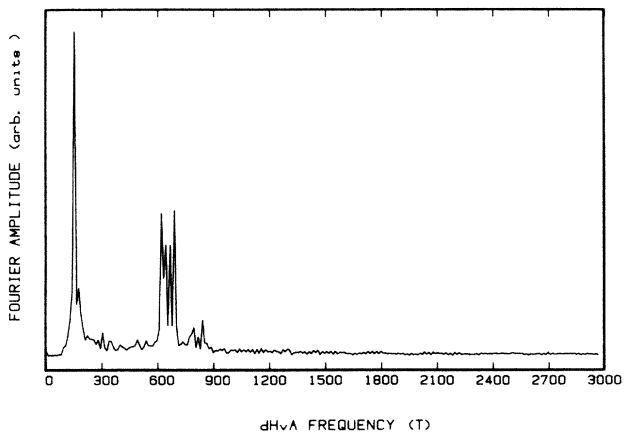

FIG. 1. Fourier transform of the dHvA signal of stage-3 $SbCl_5$-graphite for the field range 3.5–5.0 T.

The sample was put inside a set of coils which consisted of a modulation coil, a pick-up coil, and a balance coil. The set of coils was placed inside a 5.5-T superconducting solenoid. The low-frequency field-modulation technique was used to detect the dHvA oscillations with a modulation frequency of 517 Hz.

For measuring the temperature dependence, all the data were taken with the c axis of the sample parallel to the direction of the magnetic field. The cyclotron mass value was determined from the temperature dependence of the dHvA amplitude between 1.4 and 4.2 K.

For measuring the angular dependence, a toothed wheel was glued to the end of the sample holder to allow the rotation of the sample with a small screw at the end of a rod that extended to the top of the dewar. By rotating the sample holder, the angle between the magnetic field direction and the c axis of the sample was changed.

III. RESULTS AND ANALYSIS

According to Blinowski's independent-subsystem model,[12] a stage-3 compound has three valence bands and three dHvA oscillations are expected. However, Takahashi *et al.*[11] found ten dHvA frequencies in stage-3 $SbCl_5$-GIC's. Here we examine the stage-3 compound again with careful preparation of the samples and cooling rate before experiments to test Blinowski's theoretical model.

Two samples were made. The first sample was measured once and the second sample was measured more extensively. The samples were put into the dHvA holder and cooled slowly between room temperature and liquid nitrogen temperature (about three days). A strong oscillation with a frequency of 37 T is observed at low magnetic fields. In the Fourier transform of the data taken from 3.5 to 5.0 T shown in Fig. 1 one can see that there are three groups of dHvA frequencies. The first group consists of a dominant frequency 152 T and a second with frequency of 165 T. The second group and the third group consist of four and three frequencies, respectively. In each group, the amplitudes of the frequencies are not greatly different. The frequencies are 620, 644, 665, and 688 T in the second group and 782, 810, and 840 T in the third group. The average frequencies of the two groups are $\bar{F}_2 = 654$ T and $\bar{F}_3 = 811$ T.

The carrier effective masses were obtained from the temperature dependence of the dHvA amplitude between 1.4 and 4.2 K. Figure 2 shows the date for F_1 fit to the proportionality $A \propto T/\sinh(bm_cT/Bm_0)$ where A is the dHvA amplitude at temperature T and magnetic field B, m_c and m_0 are the cyclotron mass and free-electron mass, respectively, and $b = 14.69$ T K^{-1}. For the frequency 165 T in the first group the effective mass could not be determined accurately. For the second and third dHvA frequency groups, the effective masses were determined by taking the average of the effective masses of the frequencies of each group. The results are $m_1 = (0.086 \pm 0.007)m_0$, $\bar{m}_2 = (0.16 \pm 0.02)m_0$, and $\bar{m}_3$

$=(0.22\pm0.02)m_0$. The effective mass corresponding to the 37 T frequency is $(0.045\pm0.005)m_0$.

All the above results are from the second sample. The measurements from the first sample have a similar dHvA frequency distribution with three groups of frequencies and another frequency at 37 T from a strong oscillation at low magnetic fields as for the second sample. The dominant frequency in the first group is 153 T and the average frequencies for the second and third groups are 617 and 828 T, respectively. These results are within 7% of those of the second sample. The following is an analysis of the second sample.

First, the 37-T oscillation cannot be accounted for within the independent subsystem model. However, for the stage-2 $SbCl_5$-GIC, Zaleski *et al.*[15] found that, in addition to the two predicted frequencies, a strong oscillation of frequency 13 T was observed at low magnetic fields. They attributed this oscillation to macroscopic-size regions which are formed by thermal contraction of the intercalate. Antimony pentachloride and graphite have different thermal expansion coefficients. On cooling the intercalate contracts faster than the graphite and leaves macroscopic-size regions near the edges of the sample with charge transfer much lower than that in the bulk.[18] It is possible that the 37-T oscillation comes from these macroscopic-size regions.

Secondly, the splitting of the frequencies in each group means that the stage-3 compound is not as simple as the Blinowski model. Otherwise, it would give three individual dHvA frequencies for stage-3 GIC's. In the present work, several possible explanations of the splitting are considered.

The splitting of the frequencies in each group means the existence of a few similar extremal cross-sectional areas for the sample. The existence of undulation of the Fermi-surface along the k_c direction can result in several similar extremal cross-sectional areas and dHvA frequencies.

The angular dependence of the dHvA frequency can give insight into the actual shape of the Fermi structure. The cross-sectional area perpendicular to the magnetic field direction of a straight cylinder follows the relation

$$A = A_0/\cos\theta \ , \tag{1}$$

where A_0 is the cross-sectional area perpendicular to the axis of the cylinder and θ is the angle between the direction of the magnetic field and the axis of the cylinder.

In order to determine whether or not the splitting of the dHvA frequencies is from the undulation of the Fermi surface, the angular dependence of the frequencies in the first group was obtained from $\theta=0°$ to $\theta=61°$. For the second and third groups, the data are not reported because of low signal at large angles. The experimental results are presented in Fig. 3 where the values of the dominant and splitting frequencies are plotted as a function of the angle θ. The solid lines represent the predictions for a straight cylinder of the Fermi structure. One can see from Fig. 3 that the two frequencies follow a cylindrical behavior for small θ. When the angle becomes larger, both frequencies do not follow the cylindrical behavior and deviations from cylinders become larger and larger. They start to drop suddenly at $\theta=48°$ and $\theta=51°$, respectively, and this means a substantial deviation from a cylindrical fit. At $\theta=55°$ they coincide.

The data presented above bring about a possible explanation of the Fermi structure for the sample. The Fer-

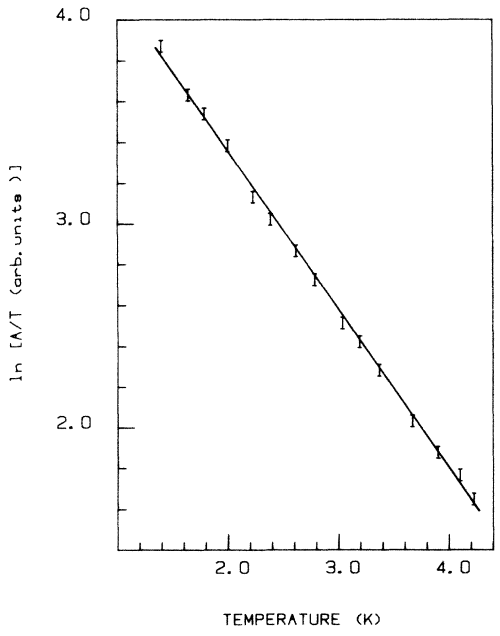

FIG. 2. Temperature dependence of A/T, where A is the amplitude of the 152-T dHvA oscillation of stage-3 $SbCl_5$-graphite measured at a magnetic field of $B=1.7$ T. The data are fitted to $A \propto T/\sinh(bm_1T/Bm_0)$ (solid line).

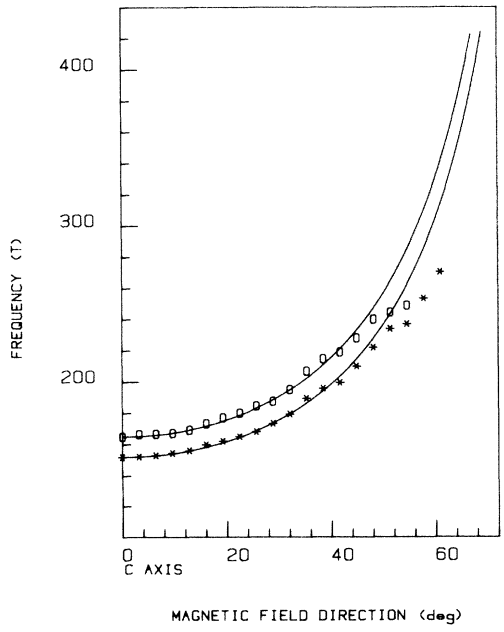

FIG. 3. dHvA frequencies 152 T (*) and 165 T (○) as a function of magnetic field direction from the c axis of stage-3 $SbCl_5$-graphite. The solid lines are cylindrical fits.

mi surface is not a straight cylinder and the fact that the difference $\Delta F\cos\theta$ gradually decreases to zero with increasing value of angle θ gives evidence of the existence of two extremal cross-sectional areas located at a maximum and minimum of the Fermi surface arising from an undulation of the Fermi surface. The actual shape of the Fermi surface could be more complicated than the description of a cylindrical Fermi surface with two extremal cross-sectional areas. The cause of some of the splitting of the second and third frequency groups could be undulation of the Fermi surface although these situations are much more complicated than the first group.

Except for the undulation of the Fermi surface, inhomogeneities in the macrostructure of the intercalant is another reason for splitting of the dHvA frequencies.

Splitting of the dHvA spectrum was also observed in stage-1 and stage-2 $SbCl_5$-GIC's.[14,15] It was reported that Blinowski's model for the stage-1 and -2 $SbCl_5$-GIC's is valid to make qualitatively predictions of the electronic properties of the GIC when the splitting of the dHvA frequencies is ignored. In fact, theoretical models usually assume a perfect system but actual experimental samples always have some kinds of defects.

Blinowski's theoretical model for a stage-3 GIC assumes that the potential energy fluctuation produced within the graphite subsystem by the charged acceptor intercalated monolayer can be neglected. This assumption is reasonable if the intercalated monolayers are basically homogeneous in distribution. When intercalated monolayers are highly inhomogeneous the potential fluctuations are not ignorable and can play a role as a perturbation to the band structure.

Levi-Setti *et al.*[19] have reported direct imaging of intercalant islands using a focused ion-beam microprobe. Thomas *et al.*[20] have observed the discontinuity of intercalant layers. Another typical evidence of inhomogeneous structure is that Hwang *et al.*[21] have observed Sb-rich islands of lateral dimension 500–1000 Å in $SbCl_5$-intercalated graphite. All these observed results show that intercalate monolayers exhibit multiphase-multidomain structure. Because the properties of the chemistry and physics of the intercalant layers directly affect the graphite-graphite or graphite-intercalant interactions, the inhomogeneities or discontinuities, particularly the domains of intercalate monolayers, can play a critical role of perturbation to these interactions and therefore affect the band structure of the GIC. Thus, the splitting of the frequencies can result from these perturbations of highly inhomogeneous structure.

In the present work, the splitting of the frequencies is time dependent. In the data taken three weeks before the data of Fig. 1 the dominant frequency of 152 T is the same. However, there are four other frequencies of 161, 169, 174, and 179 T, that is, the fresh sample has more frequencies. The phenomenon that the number of splitting frequencies decreases with time could be considered as resulting from the melting of the islands with time or a change in the number or area of islands. The melting of these islands in $SbCl_5$ graphite with time has been reported by Hwang and Nicolaides.[22]

However, no matter how complicated the reasons for the splitting of the dHvA frequencies, the important thing is that the experimental results have three dHvA frequency groups instead of two or four groups for the stage-3 sample. The three dHvA frequency groups correspond to the three individual frequencies expected from the theoretical model. The measured parameters for the groups are given in Table I. The next section is a detailed discussion of the energy bands and charge distribution of the stage-3 antimony-pentachloride graphite intercalation compound.

IV. DISCUSSION

A. Band structure of the stage-3 compound

For a stage-3 compound Blinowski's model predicts that there are three valence bands whose energies are given by

$$\begin{aligned} E_1 &= \delta - |X| \ , \\ E_2 &= -\{\delta^2+\gamma_1^2+|X|^2 \\ &\quad -[\gamma_1^4+(4\delta^2+2\gamma_1^2)|X|^2]^{1/2}\}^{1/2} \ , \\ E_3 &= -\{\delta^2+\gamma_1^2+|X|^2 \\ &\quad +[\gamma_1^4+(4\delta^2+2\gamma_1^2)|X|^2]^{1/2}\}^{1/2} \ . \end{aligned} \tag{2}$$

The Fermi areas of the bands are given by

$$\begin{aligned} A_1 &= (E-\delta)^2 \frac{\pi}{(\frac{3}{2}\gamma_0 b)^2} \ , \\ A_2 &= \{E^2+\delta^2+[4E^2\delta^2+2\gamma_1^2(E^2-\delta^2)]^{1/2}\} \frac{\pi}{(\frac{3}{2}\gamma_0 b)^2} \ , \\ A_3 &= \{E^2+\delta^2-[4E^2\delta^2+2\gamma_1^2(E^2-\delta^2)]^{1/2}\} \frac{\pi}{(\frac{3}{2}\gamma_0 b)^2} \ . \end{aligned} \tag{3}$$

Equation (2) is obtained from the three-layer Hamiltonian in the subspace spanned by the six simplest tight-binding functions. In the vicinity of the U points of the 2D Brillouin zone, $|X| = \frac{3}{2}\gamma_0 bK$, K being the distance from $\mathbf{k}$ to the U point and b is the nearest-neighbor distance. γ_0 and γ_1 are the resonance integrals. The parameter 2δ is the potential energy difference between external and internal layers. 2δ turns out to be (see the Blinowski and Rigaux[12] Appendix)

$$2\delta = 0.1 + \frac{f}{l}(57.6z - 2.7) \ (\text{eV}) \tag{4}$$

where f is the charge-transfer coefficient per intercalated molecule in the compound (C_lX) and z denotes the frac-

TABLE I. Comparison of experiment with theory.

Frequency (T)		Area (Å^{-2})		Cyclotron mass (units of m_0)	
Expt.	Calc.	Expt.	Calc.	Expt.	Calc.
152	151	0.0145	0.0144	0.086	0.097
654	653	0.0624	0.0623	0.16	0.18
811	813	0.0774	0.0776	0.22	0.21

tion of the excess charge accumulated on internal layers.

The area dependence on energy is differentiated to obtain the cyclotron mass. The cyclotron masses are given by

$$m_{c1}=\frac{\hbar^2}{(\frac{3}{2}\gamma_0 b)^2}(E-\delta)\ ,$$

$$m_{c2}=\frac{\hbar^2}{(\frac{3}{2}\gamma_0 b)^2}E\left[1+\frac{2\delta^2+\gamma_1^2}{[4E^2\delta^2+2\gamma_1^2(E^2-\delta^2)]^{1/2}}\right]\ , \tag{5}$$

$$m_{c3}=\frac{\hbar^2}{(\frac{3}{2}\gamma_0 b)^2}E\left[1-\frac{2\delta^2+\gamma_1^2}{[4E^2\delta^2+2\gamma_1^2(E^2-\delta^2)]^{1/2}}\right]\ .$$

The procedure used for calculating the theoretical parameters is as follows. From the theoretical model the Fermi areas [Eq. (3)] are calculated for various values of γ_0, γ_1, and δ, where the Fermi energy is taken as 0.71 eV from the optical reflectance study of Hoffman *et al.*[9] Choices of $\gamma_0=2.8$ eV, $\gamma_1=0.31$ eV, and $\delta=0.13$ eV make the theoretical Fermi areas in good agreement with the experimental data. Then, the values of γ_0, γ_1, and δ are used to calculate the cyclotron masses according to Eq. (5). The comparison of the experimental data to the model of Blinowski *et al.* is shown in Table I.

The validity of the model of the electronic structure of stage-3 intercalation compounds can be checked by comparing the cyclotron masses, because they are not used to determine the band structure.

The calculated cyclotron masses of $0.097m_0$ and $0.18m_0$ are 12% larger than the observed values of $0.086m_0$ and $0.16m_0$. The calculated value of $0.21m_0$ is only 5% smaller than the observed one of $0.22m_0$. This is reasonable agreement between theory and experiment. In addition calculated and measured frequencies agree very well. Thus, one can use the model of Blinowski and Regaux to make predictions of the electronic properties of the acceptor compounds.

Figure 4 shows the energy bands for the stage-3 $SbCl_5$-GIC according to Eq. (2) with $\gamma_0=2.8$ eV, $\gamma_1=0.31$ eV and $\delta=0.13$ eV. The labeled number of each band corresponds to the number of the band in Eq. (2). One can see from Fig. 4 that for stage-3 $SbCl_5$-GIC's there are three valence bands and three conduction bands. For acceptor compounds, the carriers are holes and the Fermi energy is negative with a value of 0.71 eV, which is the dashed line in Fig. 4. The differences between the bands at the Fermi level are $\Delta E_{31}=0.42$ eV and $\Delta E_{32}=0.51$ eV. Here, ΔE_{32} is the energy difference between valence bands 3 and 2, and ΔE_{31} is the energy difference between valence bands 3 and 1. The optical reflectance study of the electronic structure of $SbCl_5$-GIC's by Hoffman *et al.*[9] reported that for the stage-3 $SbCl_5$-GIC the values of energy-band differences are $\Delta E_{31}=0.40$ eV and $\Delta E_{32}=0.56$ eV. Thus the band energy differences from this work are 5% larger in ΔE_{31} and 10% smaller in ΔE_{32} than the optical experimental results. This is considered good agreement of band energy differences and proves that Blinowski's theoretical model for the stage-3 GIC is reasonable and that the values of the band parameters γ_0, γ_1, and δ are suitable.

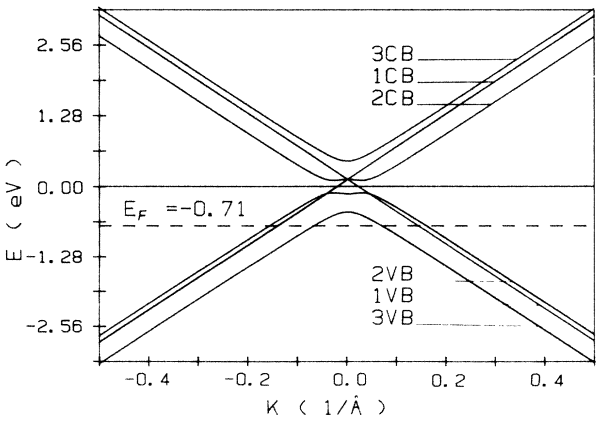

FIG. 4. The band structure near the U point of stage-3 $SbCl_5$-graphite for $\delta=0.13$, $\gamma_0=2.8$, $\gamma_1=0.31$.

The parameters γ_0 and γ_1 are two important values which indicate the interactions of nearest neighbors and nearest layers. For pristine graphite, the values of γ_0 and γ_1 are 3.16 and 0.39 eV, respectively.[23] For the first and second stages of $SbCl_5$-GIC's, by using the Fermi energies from optical experiments[9] and by referencing the dHvA frequencies,[14,15] the value of γ_0 for the stage-1 $SbCl_5$-GIC was taken to be 2.4 eV and the values of γ_0 and γ_1 for the stage-2 $SbCl_5$-GIC are 2.67 eV and 0.38 eV, respectively. For the stage-3 $SbCl_5$-GIC, from the present work, the values of γ_0 and γ_1 are 2.8 and 0.31 eV. γ_0 increases with stage number and becomes closer to pristine graphite as the number of layers increases and the interaction between nearest neighbors increases. The deviations from the graphitic value of γ_0 in the graphite intercalation compounds comes from the effect of the higher-order terms in the Hamiltonian. The effective value of the γ_0 parameters behaves as predicted: the larger the Fermi surface the lower the value of γ_0.[12,13] The interaction between nearest layers is also different from pristine graphite but, as indicated by the values of γ_1, there is no systematic variation with stage number.

B. Charge transfer

The total charge per carbon atom can be expressed by[24]

$$\frac{f}{l}=\frac{a^2\sqrt{3}}{4\pi^2 n}\sum_i A_{Fi}\ , \tag{6}$$

where f is the charge transferred per intercalated molecule, l is the number of carbon atoms for each intercalate molecule, n is the stage number, a is the length of the primitive lattice translation vector, and A_{Fi} is the Fermi surface cross-sectional area perpendicular to the k_z direction. The area A_{Fi} is directly proportional to the dHvA frequency. Thus, the dHvA effect measures the charge transfer directly.

The sum of the dHvA frequencies in stage 3 is 1622 T and is almost identical in stage 2 with 1615 T. This means that the charge transfer per intercalant is the same in both stages. It follows that the charge transfer is the same in stages 2 and 3 (and has to be so in higher stages) and is lower only in stage 1. That is, the saturation of the charge transfer occurs after stage 1.

For the present work, n is equal to 3, and the sum of the dHvA frequencies is 1622 T. The total charge per carbon atom from Eq. (6) is then 0.0137. The stage-3 $SbCl_5$-GIC expressed by $C_{36}SbCl_5$ gives the number l as 36. Thus the charge f, transferred from carbon atoms to each intercalated $SbCl_5$ molecule, is found to be 0.493. This result is in agreement with the result of Takahashi *et al.*,[11] who found that the amount of charge transfer per intercalant is 0.49 for the stage-3 $SbCl_5$-GIC.

Having the value of charge transfer per carbon atom f/l, one can calculate the fraction of the excess charge accumulated on the internal layer by Eq. (4). For a uniform charge distribution,[25] z is $\frac{1}{3}$ for stage 3. For another extreme case, the metallic sandwich model,[10] z is zero. In the present work, δ is equal to 0.13 eV, and f/l is equal to 0.0137, the value of z is 0.25. This value of z is larger than zero and smaller than $\frac{1}{3}$. That is, it is between the uniform charge distribution model and the metallic sandwich model and there is a deficiency of charge on the internal graphite layer relative to the layers next to the intercalant.

This experimental result of the charge distribution can be compared with the theoretical calculation by Pietronero *et al.*,[26] who applied the Thomas-Fermi model to calculate the excess charge distribution among the different graphite layers in a lameller graphite acceptor compound. Their calculated results show that the charge distribution along the c direction is inhomogeneous. By using the value of $f=0.493$ from the present work, the value of z for the stage-3 $SbCl_5$-GIC is calculated as 0.224. This value is very close to our value of $z=0.25$. Thus, the experimental and theoretical results for the charge distribution illustrate that, in a stage-3 acceptor compound, the charge distribution among the three graphite layers is not as simple as a metallic sandwich model or a homogeneous charge distribution model. The charge on the internal graphite layers is less than that on the external graphite layers. This situation of an inhomogeneous charge distribution results from an effective screening of the internal layer by the external graphite layers.

V. CONCLUSIONS

Samples of the stage-3 antimony-pentachloride graphite intercalation compound were prepared by a two-zone method. The stage index was determined by x-ray diffraction. The electronic properties of the $SbCl_5$-GIC were carefully studied by means of the de Haas–van Alphen effect after cooling the samples slowly. The experimental results include the angular dependence of the dHvA frequency distribution and the accurate frequencies and the temperature dependence of the dHvA amplitude with the magnetic field parallel to the c axis of the samples.

The de Haas–van Alphen measurements with the magnetic field direction parallel to the c axis show three groups of dHvA frequencies. The dominant frequency from the first group and the two average frequencies from the second and third groups are identified with the basic graphite bands. The splitting of the frequencies is attributed to two reasons. The first is the undulation of the Fermi surface along the k_z direction as determined from the angular dependence. The second is the existence of intercalate islands which produce a perturbation affecting the interactions of graphite-graphite or graphite-intercalant. In addition, the splitting of the frequencies is time-dependent which could result from the instability of intercalant islands in the samples.

The experimental dHvA frequencies are used to determine the band parameters γ_0, γ_1, and δ in Blinowski's theoretical band model for the stage-3 $SbCl_5$-GIC. The value of the parameter γ_0, which indicates the interaction of nearest neighbors, is higher than the values of stage-1 and stage-2 $SbCl_5$-GIC's.[14,15] The value of γ_0 actually increases with stage number and tends to the value of pristine graphite. The value of the parameter γ_1, which indicates the interaction of nearest layers, changes irregularly with stage number.

The three parameters γ_0, γ_1, and δ are then returned to Blinowski's energy-band equations[12] to calculate cyclotron masses and band energy differences. The measured cyclotron masses are determined from the temperature dependence of the dHvA amplitude. The values of the measured cyclotron mass for the first frequency and the average measured cyclotron masses for the second and third groups agree with the three values of Blinowski's theoretical predictions. The energy differences between the valence bands around the Fermi level are in agreement with the optical reflectance experimental results of Hoffman *et al.*[9]

The charge transfer coefficient per intercalant is determined from the observed sum of the dHvA frequencies. This coefficient and another band parameter δ which is associated with the excess charge distribution are used to find the fractional charge distribution of the three graphite layers along the k_z direction. The fractional charge distribution from Blinowski's model agrees with the calculation for a stage-3 GIC by Pietronero *et al.*[26] Both experimental and calculational results for the fractional charge distribution show that there is a deficiency of charge in the internal graphite layer relative to the layers next to the intercalant. This is between the uniform charge distribution model and the metallic sandwich model. This situation results from the screening effect of the external graphite layers which are adjacent to the intercalate layers.

ACKNOWLEDGMENTS

We wish to thank Dr. A. W. Moore for the HOPG graphite and T. Olech for technical assistance. The research was supported by the Natural Sciences and Research Council of Canada.

[1]V. R. K. Murthy, D. S. Smith, and P. C. Eklund, Mater. Sci. Eng. **49**, 455 (1982).
[2]J. Melin and A. Herold, Carbon **13**, 357 (1975).
[3]J. Melin and A. Herold, C. R. Acad. Sci. Paris **269**, 877 (1969).
[4]V. R. K. Murthy, D. S. Smith, and P. C. Eklund, Mater. Sci. Eng. **49**, **45**, 77 (1980).
[5]H. Homma and R. Clarke, Phys. Rev. B **31**, 5865 (1985).
[6]L. Salamanca-Riba, G. Roth, J. M. Gibson, A. R. Kortan, G. Dresselhaus, and R. J. Birgeneau, Phys. Rev. B **33**, 2738 (1986).
[7]G. Timp, M. S. Dresselhaus, L. Salamanca-Riba, A. Erbil, L. W. Hobbs, G. Dresselhaus, P. C. Eklund, and Y. Iye, Phys. Rev. B **26**, 2323 (1982).
[8]Y. Yosida, S. Tanuma, S. Takagi, and K. Soto, in *Graphite Intercalation Compounds,* Vol. 51 of *Materials Research Society Extended Abstracts,* edited by P. C. Eklund, M. S. Dresselhaus, and G. Dresselhaus (MRS, Boston, 1984).
[9]D. M. Hoffman, R. E. Heinz, G. L. Doll, and P. C. Eklund, Phys. Rev. B **32**, 1278 (1985).
[10]F. Batallan, J. Bok, I. Rosenman, and J. J. Melin, Phys. Rev. Lett. **41**, 330 (1978).
[11]O. Takahaski, Y. Iye, and S. Tanuma, Solid State Commun. **37**, 863 (1981).
[12]J. Blinowski and C. Rigaux, J. Phys. (Paris) **41**, 667 (1980).
[13]J. Blinowski, H. H. Nguyen, C. Rigaux, J. P. Vieren, R. Letoullec, G. Furdin, A. Herold, and J. J. Melin, J. Phys. (Paris) **41**, 47 (1980).
[14]H. Zaleski, P. K. Ummat, and W. R. Datars, J. Phys. C **17**, 3167 (1984).
[15]H. Zaleski, P. K. Ummat, and W. R Datars, Phys. Rev. B **35**, 2958 (1987).
[16]N. A. W. Holzwarth, Phys. Rev. B **21**, 3665 (1980).
[17]Y. Yosida and S. Tanuma, J. Phys. Soc. Jpn. **54**, 701 (1985); **54**, 707 (1985).
[18]L. E. McNiel, J. Steinbeck, L. Salamanca-Riba, and G. Dresselhaus, Phys. Rev. B **31**, 2451 (1985).
[19]R. Levi-Setti, G. Cron, Y. L. Wang, N. W. Parker, and R. K. Mittleman, Phys. Rev. Lett. **54**, 2615 (1985).
[20]J. M. Thomas, G. R. Millward, R. F. Schlogl, and H. P. Boehm, Mater. Res. Bull. **15**, 671 (1980).
[21]D. M. Hwang, X. W. Qian, and S. A. Solin, Phys. Rev. Lett. **53**, 1473 (1984).
[22]D. M. Hwang and G. Nicolaides, Solid State Commun. **49**, 483 (1984).
[23]M. S. Dresselhaus, and G. Dresselhaus, Adv. Phys. **30**, 139 (1981).
[24]H. Zaleski, P. K. Ummat, and W. R. Datars, Synth. Met. **11**, 183 (1985).
[25]M. S. Dresselhaus, G. Dresselhaus, and J. E. Fischer, Phys. Rev. B **15**, 3180 (1977).
[26]L. Pietronero, S. Strassler, and H. R. Zeller, Phys. Rev. Lett. **41**, 763 (1978).